*Am J Physiol Heart Circ Physiol* 293: H1526–H1535, 2007.
First published May 25, 2007; doi:10.1152/ajpheart.01090.2006.

# Temporal and spatial variations of cell-free layer width in arterioles

**Sangho Kim,[1,3] Robert L. Kong,[1] Aleksander S. Popel,[2] Marcos Intaglietta,[1] and Paul C. Johnson[1]**

[1]*Department of Bioengineering, University of California, San Diego, La Jolla, California;* [2]*Department of Biomedical Engineering, Johns Hopkins University, Baltimore, Maryland; and* [3]*Division of Bioengineering, National University of Singapore, Singapore*

Submitted 5 October 2006; accepted in final form 21 May 2007

**Kim S, Kong RL, Popel AS, Intaglietta M, Johnson PC.** Temporal and spatial variations of cell-free layer width in arterioles. *Am J Physiol Heart Circ Physiol* 293: H1526–H1535, 2007. First published May 25, 2007; doi:10.1152/ajpheart.01090.2006.—Separation of red blood cells and plasma in microcirculatory vessels produces a cell-free layer at the wall. This layer may be an important determinant of blood viscosity and wall shear stress in arterioles, where most of the hydraulic pressure loss in the circulatory system occurs and flow regulatory mechanisms are prominent. With the use of a newly developed method, the width of the cell-free layer was rapidly and repeatedly determined in arterioles (10- to 50-μm inner diameter) in the rat cremaster muscle at normal arterial pressure. The temporal variation of the cell-free layer width was non-Gaussian, but calculated mean and median values differed by <0.2 μm. The correlation length of the temporal variations downstream (an indication of mixing) was ~30 μm and was independent of pseudoshear rate (ratio of mean velocity to vessel diameter) and of vessel diameter. The cell-free layer width was significantly different on opposite sides of the vessel and inversely related. Increasing red blood cell aggregability reduced this inverse relation but had no effect on correlation length. In the diameter range studied, the mean width of the cell-free layer increased from 0.8 to 3.1 μm and temporal variations increased from 30% to 70% of the mean width. Increased aggregability did not alter either relationship. In summary, the cell-free layer width in arterioles is diameter dependent and shows substantial non-Gaussian temporal variations. The temporal variations increase as diameter increases and are inversely related on opposite sides of the vessel.

plasma layer; correlation length; red blood cell; aggregation; hemorheology

PHASE SEPARATION OF RED BLOOD cells and plasma leads to formation of a cell-free or cell-poor layer adjacent to the endothelium in arterioles and venules. This phenomenon is attributed to axial migration of red blood cells. It has been shown experimentally and theoretically that increasing the width of the layer reduces the effective viscosity of blood (8, 10, 38). A recent theoretical study showed that an irregular boundary between the central red blood cell core and the plasma layer tends to diminish this effect of the cell-free layer on effective blood viscosity (40). Thus it appears that both the mean width and its variations may contribute to effective blood viscosity.

The cell-free layer may contribute importantly to microvascular function since effective blood viscosity and wall shear rate determine wall shear stress. Wall shear stress is one of the principal stimuli for release of the vasodilators, nitric oxide (NO), and prostaglandins by the endothelium (5, 23). The cell-free layer also acts as a barrier to NO scavenging by the red blood cell core. A study on 60-μm isolated arterioles (25) showed that, when blood flowed through the vessel, there was almost no NO scavenging effect on the arteriolar wall, whereas during flow stasis there was a large effect. The difference is presumably due to formation of the cell-free layer during flow. In addition, studies in which hemoglobin perfusion solutions have been used as a blood substitute have shown a strong vasoconstrictor effect, which is attributed to NO scavenging at the vessel wall (33). Theoretical studies also provide evidence that an inverse relation exists between the cell-free layer width and the scavenging effect of red blood cells in the flow stream on the NO produced by the endothelial layer (6, 7, 19, 24, 47).

However, data on the cell-free layer width in the microcirculation are very limited. Yamaguchi et al. (49) reported that the width of the cell-free layer in cat cerebral microvessels [34- to 56-μm inner diameter (ID)] was ~4 μm and independent of vessel diameter, whereas Maeda and coworkers (43) reported that the width of the layer in vessels of 10- to 40-μm ID was ~1 to 2 μm with a suspension of human red blood cells in saline perfused through the rabbit mesentery, and the value was diameter dependent. These reports were based on visual estimates with a calibrated eyepiece or manual measurement from videotape replay. Pries et al. (35) obtained a cell-free layer width of 1.6 ± 1.3 μm (mean ± SD) from studies of phase separation at arteriolar bifurcations, and the value was also diameter dependent.

We (20) have recently developed a computer-based method for monitoring the width of the cell-free layer in vivo in conjunction with a high-speed video camera that enables measurements at a rate of up to 4,500 frames/s. This method provides information on mean width and on variations from frame to frame at a single site and enables comparisons among sites within the same microscopic field. These features of the method enable us to examine issues such as the axisymmetry of the flow stream and the interdependence of layer width at adjacent sites in individual vessels.

The region of the peripheral circulation where the cell-free layer may have the greatest effect on function is the arteriolar network because this is the area where shear stress is greatest, most of the pressure drop occurs, and flow regulatory mechanisms are most prominent (18, 27). We were particularly interested in determining *1*) the actual width of the cell-free layer since this influences both the effective blood viscosity and NO scavenging by the red blood cell core, *2*) the relation, if any, between the layer width and vessel diameter, *3*) the degree of variation in the layer width because this may influ-

Address for reprint requests and other correspondence: P. C. Johnson, Dept. of Bioengineering, Univ. of California, San Diego, La Jolla, CA 92093-0412 (e-mail: pjohnson@bioeng.ucsd.edu).

The costs of publication of this article were defrayed in part by the payment of page charges. The article must therefore be hereby marked "*advertisement*" in accordance with 18 U.S.C. Section 1734 solely to indicate this fact.

ence both effective viscosity and NO scavenging, *4*) the axisymmetry of the cell-free layer on opposite sides of the vessel because this influences effective viscosity, and *5*) the persistence of the cell-free layer form and dimensions downstream because this reflects the degree of mixing between the layer and the red blood cell core. Finally, to relate our findings more closely to humans, the studies were repeated after increasing red blood cell aggregability to the level seen in normal humans by infusion of a high-molecular-weight polymer. All experiments were carried out at normal arterial pressure.

## MATERIALS AND METHODS

### *Animal Preparation*

A total of 11 Wistar-Furth rats weighing between 190 and 250 g were used in this study. Animals were anesthetized with 50 mg/kg ip pentobarbital sodium, with additional anesthetic administered throughout the experiment as needed. The animal was placed on a heating pad to maintain body temperature at 37°C during surgery and the experiment, and a tracheal tube was inserted to aid ventilation. All procedures were in accordance with the *Guide for the Care and Use of Laboratory Animals* (Institute for Laboratory Animal Research, National Research Council, Washington, DC: National Academy Press, 1996) and approved by the local Animal Subjects Committee. The femoral artery was catheterized for blood withdrawals and pressure measurements, and the jugular vein was catheterized for administration of anesthetic, dextran 500 (average molecular mass of 460 kDa; Sigma) dissolved in saline (6%), and other solutions. All catheters were filled with a solution of heparinized saline (30 IU/ml) to prevent clotting.

The exteriorized rat cremaster muscle preparation was used for microcirculatory studies (1). After surgical exposure of the muscle, a drip of warm Plasma-Lyte A (Baxter) adjusted to pH 7.4 was applied while connective tissue was cleared and the muscle was separated from the surrounding tissue with the nerves and blood supply intact. The animal was then placed on a Plexiglas plate, and the muscle was secured to a platform for viewing, suffused with Plasma-Lyte A, and covered with polyvinyl film. Muscle temperature was maintained at 35°C with heating coils beneath the plate and the muscle platform.

### *Hematocrit, Aggregation, and Systemic Cardiovascular Measurements*

The hematocrit was determined with a microhematocrit centrifuge (Readacrit, Clay Adams) and degree of red blood cell aggregation with an aggregometer (Myrenne aggregometer; Myrenne, Roetgen, Germany) periodically during the experiments. Arterial pressure in the femoral artery was obtained with a physiological data-acquisition system (MP 100 System; BIOPAC Systems, Goleta, CA).

### *Experimental Protocol*

After the animal had been mounted on the microscope stage and a period of ~20 min allowed for stabilization, an arterial blood sample was taken to determine control values of hematocrit and aggregation index. Next, an unbranched region of an arteriole in the range of 10–50 μm ID was selected for study based on the criteria of stable flow, clear focus, and contrast of the image. Vessels in this diameter range are responsible for a substantial portion of total vascular resistance (26, 34). An intravital microscope (Ortholux II, Leitz) was used with an Olympus ×40 water-immersion objective and a long working distance condenser (Instec, Boulder, CO), which have numerical apertures of 0.7 and 0.35, respectively. A blue filter with peak transmission at 400 nm (Spectra Physics, no. 59820) was placed before the light source to maximize light absorption by the red blood cells.

The microscope was focused on the equatorial plane of the arteriole, and the video image was recorded at a rate of 4,500 frames/s. After this recording was completed, dextran 500 was infused to induce red blood cell aggregation at the levels seen in blood of healthy humans. A total of 200 mg/kg body wt was infused over the course of 1–2 min to achieve an estimated plasma dextran concentration of ~0.6%. After ~10 min, an additional blood sample was taken to determine hematocrit and aggregation index. Additional dextran was given if needed to achieve an aggregation index value with the Myrenne aggregometer similar to the levels (12–16) of normal human blood (22, 31, 50). The video recording procedure was then repeated at the same vessel site.

### *Image Analysis*

*Cell-free layer determination.* An analysis line was placed across the vessel perpendicular to vessel wall using SigmaScan Pro 5 software. To position the line exactly perpendicular to the vessel wall, a five-pixel line parallel to the vessel wall at a point of interest was drawn. The analysis line was placed at the midpoint of the 5-pixel line, perpendicular to it, and at least two vessel diameters away from the nearest upstream bifurcation. The width of the cell-free layer was determined from the position of the vessel wall and the outer edge of the red blood cell core. We followed criteria used in previous studies (13, 42, 48) in determining vessel wall location. The edge of the red blood cell core was determined by Otsu's method as previously described (20). In the present study, the spatial resolution of the cell-free layer measurement was ~0.4 μm. Detailed information on the method for determination of the cell-free layer width is described in our earlier study (20). In most instances, the width of the cell-free layer on the opposite side of the vessel was also determined.

*Mean velocity and pseudoshear rate.* The centerline velocity in the arterioles was determined by the dual-window method from the high-speed video recordings using a video sampler and velocity correlator system (2, 15). The mean velocity ($V_{mean}$) was determined from the relationship $V_{mean}$ = centerline velocity/1.6, where 1.6 is a correction factor (2), whereas the pseudoshear rate was determined from the following relationship: pseudoshear rate = $V_{mean}/D$, where $D$ is vessel diameter.

*Typical correlation length of cell-free layer.* To determine the persistence of the cell-free layer pattern downstream, cell-free layer data were obtained at two points along the length of the vessel on one side. The first line was established as the baseline (*line 1*). As shown in Fig. 1, *line 2* was placed at a distance $x$ from the baseline. Values of $x$ of 0.25$D$, 0.5$D$, 0.75$D$, 1$D$, 1.5$D$, 2$D$, and 3$D$, with $D$ representing the diameter of the vessel under analysis, were used. The cell-free layer width over a period of 1 s from each position of *line 2* on one side of the vessel was cross-correlated against the baseline measurement on the same side using a signal-processing software package (MATLAB, Mathworks, Natick, MA). To normalize the correlation peak, the autocorrelation of *line 1* was used. The correlation values were plotted against the distance between *line 1* and *line 2* and an exponential curve fitted to the data, with the $y$-intercept being set to unity. The correlation length was then determined as described by Silva and Intaglietta (41). With the assumption that the normalized peak-correlation coefficient, $f_c(x)$, is an exponentially decreasing function of analysis line separation, $x$, $f_c(x)$ was defined as follows:

$$f_c(x) = e^{-kx} \text{ for } 0 \le x \le \infty$$
$$f_c(x) = 0 \text{ for } x < 0 \quad (1)$$

Then $\int_0^\infty f_c(x)dx = 1/k$, and the correlation length is defined as the downstream distance $x$, where $x = 1/k$ or where the normalized correlation coefficient has decreased to $1/e$ (0.368).

*Width correlation on opposite sides of the arterioles.* A correlation analysis of the cell-free layer width on opposite sides of the vessel was also performed. For this analysis, variations of the cell-free layer width at $A$ and $A'$ as shown in Fig. 1 were compared. The degree of

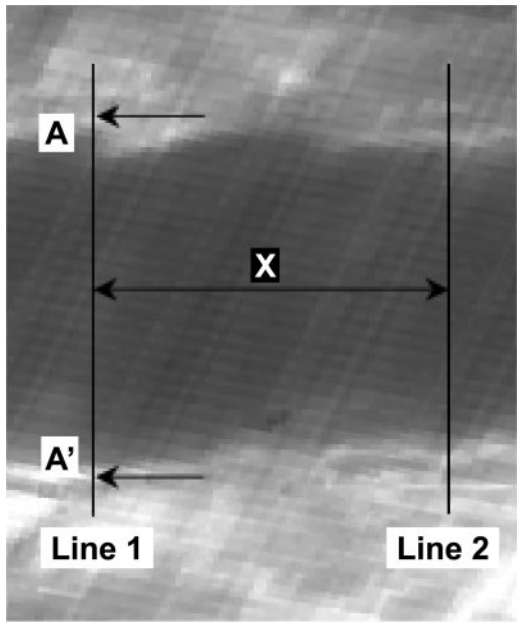


Fig. 1. Cell-free layer width determination by a computer-based method (17). Videomicrograph of red blood cell flow in an arteriole [41-μm inner diameter (ID)] after dextran infusion with 2 analysis lines is shown. Arrows indicate the location of the inner margin of the vessel wall. See text for details of analysis.

correlation between the variations in the width at the two sites was determined by nonparametric Spearman correlation analysis. The Spearman coefficient ($R_s$) ranges from 1 to −1, with $R_s = 1$ representing a perfect direct correlation and $R_s = -1$ a perfect inverse correlation.

### *Statistical Analysis*

A statistical software package (Prism 4.0, GraphPad) was used for statistical analyses including regression analysis. We utilized unpaired *t*-tests to determine experimental and physiological parameters between normal and dextran-treated rats. For a normality test, we used the one-sample Kolmogorov-Smirnov test. In cases where data did not follow a Gaussian distribution, a nonparametric test (Mann-Whitney test) and unpaired *t*-tests were used to compare medians and means, respectively. However, with large samples ($n > 100$), parametric tests such as *t*-tests are as accurate as nonparametric tests (32). Because $n > 4{,}000$ in the present study, a Gaussian distribution was not required for the comparison of the data groups.

All physiological and rheological values are reported as means ± SD, and the cell-free layer width medians are reported as well. $P < 0.05$ was considered statistically significant for all tests and regression fits.

## RESULTS

### *Systemic Variables and Arteriolar Flow*

Arterial pressure was 117 ± 8 and 112 ± 7 mmHg and the systemic hematocrit was 42 ± 2% and 41 ± 2% before and after dextran infusion, respectively. We found no significant effects of dextran 500 on arterial pressure or systemic hematocrit. The index of aggregation as determined with the Myrenne aggregometer was 0.0 before and 13.7 ± 1.1 after induction of aggregation.

$V_{mean}$ of red blood cells was 8.6 ± 2.5 and 6.8 ± 2.9 mm/s before and after dextran infusion, respectively, leading to volume flow rates of 8.2 ± 5.1 and 7.7 ± 6.4 nl/s. Neither of these differences was significant. We found no significant difference in pseudoshear rates before (288.2 ± 150.5 $s^{-1}$) and after (220.3 ± 123.4 $s^{-1}$) infusion. Although the data shown in Fig. 2 suggest a trend, we found no significant relation between the pseudoshear rate and arteriolar diameter either before or after dextran 500. However, when the two groups were combined, there was a significant inverse relation. In general, mean cellular velocity was directly related to arteriolar diameter. However, this effect was small compared with the change in diameter, creating an inverse relation between pseudoshear rate and diameter as shown in Fig. 2.

### *Variations in Cell-Free Layer Width*

Measurements of the cell-free layer width show substantial temporal variations. An example of the cell-free layer width on opposite sides of a 41-μm ID arteriole (A and A′) is shown in Fig. 3*A*. Rapid variations in the width of the cell-free layer are apparent on both sides of the arteriole with greater variations from the mean width inward to the red blood cell column than outward toward the vessel wall. Also, occasionally, the red blood cell column appears to extend to the vessel wall. The frequency distributions of cell-free layer width at A and A′ are shown in Fig. 3*B*. From visual inspection of Fig. 3*B*, it appears that the distributions are non-Gaussian. In fact, width distribution in all arterioles ($n = 21$) failed the normality test ($P < 0.0001$).

### *Comparison of the Cell-Free Layers on the Two Sides of the Vessel*

It is evident in Fig. 3*C* that the mean width of the cell-free layer is substantially different on the two sides of this particular vessel. Statistical comparison of the two cell-free layers for all arterioles shows that both the mean and median values of the cell-free layer width measured over a 1-s period ($n = 4{,}500$) were significantly different on opposite sides of the vessels ($P < 0.0001$). The difference in the means on the two sides was 0.5 ± 0.4 μm before dextran infusion and was not significantly affected by dextran, being 0.6 ± 0.5 μm after infusion. In

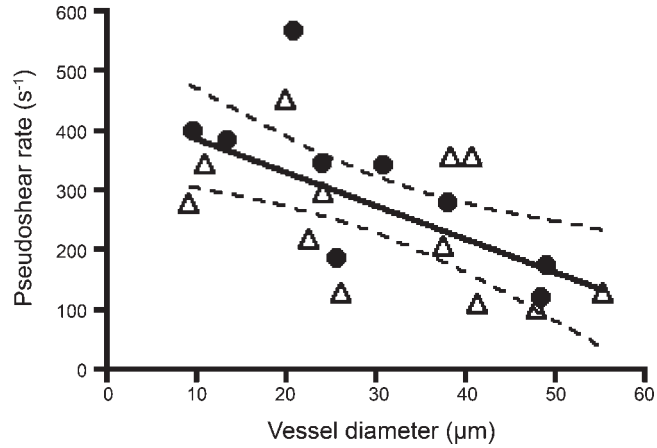


Fig. 2. Pseudoshear rate vs. vessel diameter. The solid line represents a linear regression curve ($y = -5.6x + 442.9$; $R^2 = 0.38$) for the combined group before (●) and after (△) dextran infusion. The dashed lines indicate the 95% confidence band of the regression line. There was a significant relation ($P < 0.05$) between pseudoshear rate and vessel diameter for the combined group but not for the 2 groups separately.

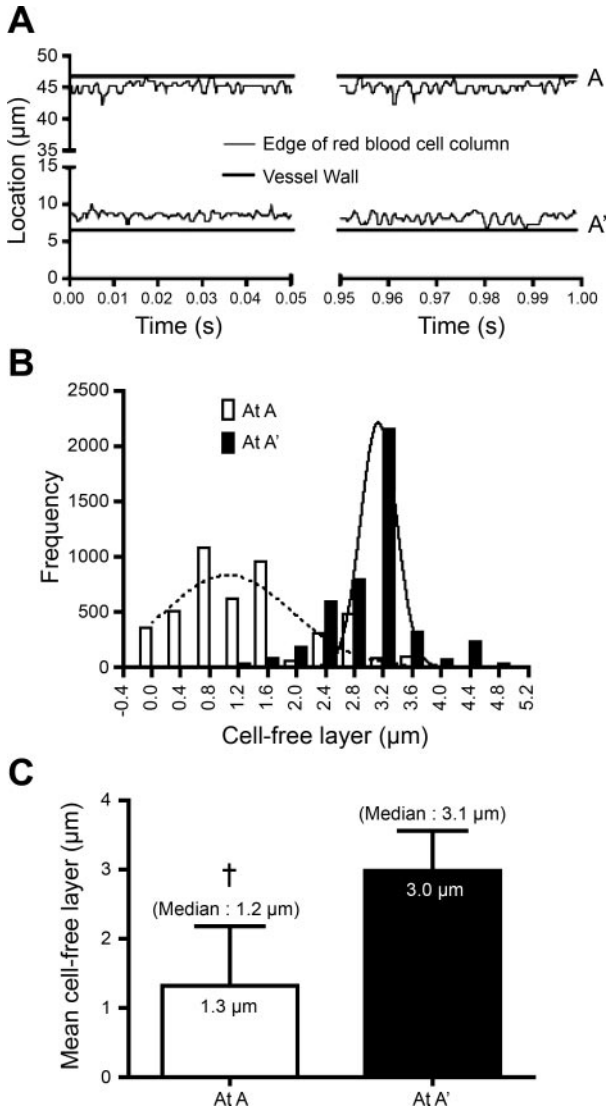


Fig. 3. Comparison of cell-free layer width variation at 2 sites (at A and A′). *A*: cell-free layer width variation at 2 sites on opposite sides of a 41-μm ID arteriole. *B*: frequency distribution of the cell-free layer width at the 2 sites. The dashed and solid curves represent best Gaussian fits to the width distributions at sites A and A′, respectively. Neither distribution passed a normality test ($P < 0.0001$). *C*: mean and median values of the cell-free layer width on the 2 sides of the vessel. There are highly significant differences in the means and in the medians of the cell-free layer widths at the 2 sites. †$P < 0.0001$.

addition, comparing instantaneous values with the nonparametric $R_s$ revealed a significant inverse relationship between the widths on the two sides ($P < 0.01$). This was evident both before and after dextran infusion. However, as shown in Fig. 4, the nonparametric $R_s$ was significantly higher before ($-0.12 \pm 0.055$) than after ($-0.03 \pm 0.055$) dextran infusion ($P < 0.02$), indicating that dextran 500 significantly decreases the asymmetry of the lateral position of the red blood cell core.

### *Persistence of the Temporal Variation Pattern Downstream*

Because the interface between the red blood cell column and the cell-free layer is a region of high shear rate in the flow stream, the extent to which these variations were maintained downstream was of particular interest. The persistence was evaluated from cross-correlation analysis of two analysis lines with separations of 0.25 to 3 vessel diameters. Figure 5*A* shows an example of normalized cross-correlation coefficients with $x = 0.5D$ and $2D$ in a 21-μm ID arteriole after dextran infusion. The correlation coefficient followed an exponential decay as a function of distance, as shown in Fig. 5*B*. The distance at which the correlation coefficient fell to $1/e$ represents the correlation length, a measure of how well the structure of the interface between the red blood cell column and the cell-free layer is maintained.

Figure 6 shows the correlation length of the cell-free layer as a function of vessel diameter and pseudoshear rate. The analysis was limited to arterioles in which we could obtain the correlation coefficient for at least two vessel diameters from the baseline ($n = 10$). The correlation length was $32.4 \pm 5.6$ and $29.7 \pm 4.0$ μm before and after dextran infusion, respectively, with no significant effect of dextran treatment. Thus the correlation length appears to be ~30 μm and independent of vessel diameter (Fig. 6*A*). Although there appears to be a slight trend toward a relation to pseudoshear rate (Fig. 6*B*), the change was not significant whether tested separately before and after dextran infusion or for the two groups combined.

### *Cell-Free Layer Width as a Function of Diameter*

One of the factors that would be expected to influence cell-free layer width is vessel diameter. The results of this comparison are presented in Fig. 7. As shown in Fig. 7*A*, the mean width of the cell-free layer increased severalfold, from 0.8 to 2.9 μm before dextran infusion and from 0.8 to 3.1 μm after dextran infusion, over the diameter range 10–50 μm. The median cell-free layer width (not shown) also significantly increased as a function of diameter from 0.7 to 2.9 μm before dextran and from 0.8 to 2.9 μm after dextran. The changes in both conditions were highly significant ($P < 0.0001$). Figure 7*B* shows the temporal variation for each vessel and represents the SD of cell-free layer during the 1-s period of width measurement. Although the variation changed to a lesser degree than width, it also increased significantly ($P < 0.05$) from 0.6 to 1.0 μm over the diameter range before dextran infusion and from 0.5 to 0.9 μm after infusion. Dextran 500 had no effect on the diameter dependence of the mean or variability.

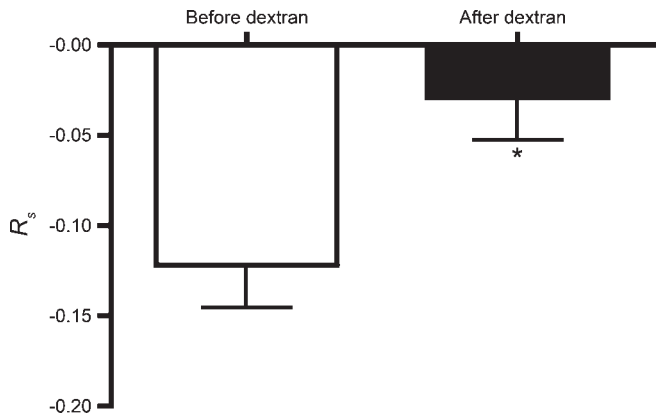


Fig. 4. Inverse relation between the widths on the 2 sides of the vessel for all arterioles ($n = 21$). The negative Spearman coefficient ($R_s$) represents the degree of inverse relationship between the instantaneous widths on the 2 sides. Note that there was a significant reduction in the inverse relation before and after infusion of dextran. *$P < 0.02$.

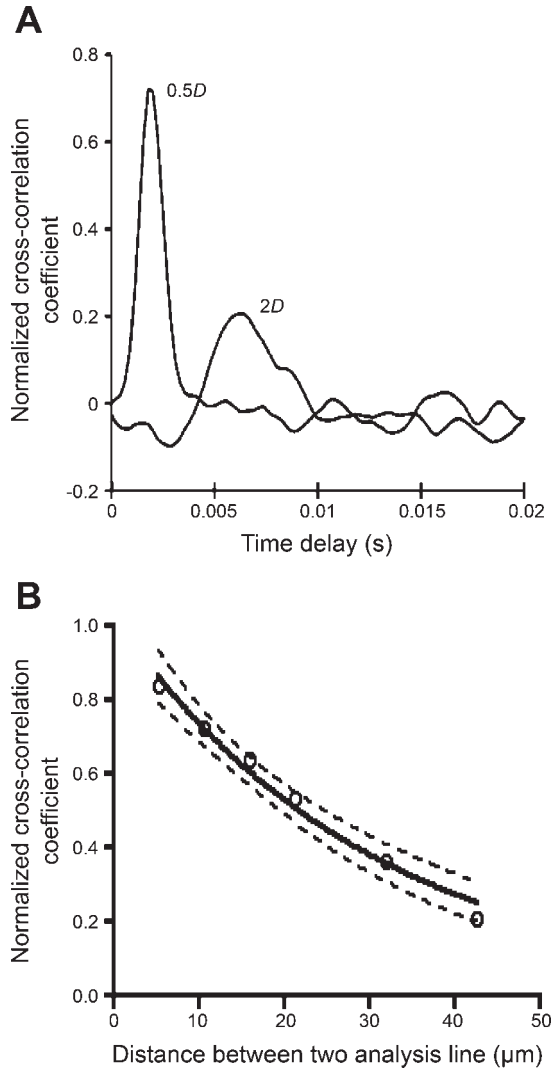


Fig. 5. Cross-correlation analysis of cell-free layer width variation. *A*: examples of normalized cross-correlation coefficient determination at 0.5*D* and 2*D*, where *D* is diameter, from the baseline in a 21-μm ID arteriole after dextran infusion. *B*: normalized cross-correlation coefficient as a function of distance from the baseline in the same arteriole. The solid line represents an exponentially decaying regression curve ($y = 1.025e^{-0.033x}$; $R^2 = 0.985$). Dashed lines indicate the 95% confidence band. The 6 coefficient points shown in *B* were obtained at 0.25*D*, 0.5*D*, 0.75*D*, 1*D*, 1.5*D*, and 2*D*, respectively, from the baseline.

### *Cell-Free Layer Width as a Function of Pseudoshear Rate*

The relations between the pseudoshear rate and the width and variation of the cell-free layer are shown in Fig. 8. The mean and variability of the cell-free layer width showed a tendency toward an inverse relation to pseudoshear rate, but the relation was not significant when tested separately before and after dextran infusion. However, the inverse relation to pseudoshear rate became significant ($P < 0.03$) when the two groups were combined. Dextran 500 had no effect on the relation between pseudoshear rate and the cell-free layer.

## DISCUSSION

As described in the introduction, there is mounting evidence that the cell-free layer may contribute importantly to the function of arterioles. This study provides new information on several questions, including the relation between the width of the layer and vessel diameter, magnitude of variations in the layer width, the effect of these variations on axisymmetry of the flow stream and on downstream sites in the vessel, and the effects of the level of red blood cell aggregability seen in normal humans on the cell-free layer. The data were obtained on 10- to 50-μm arterioles and as such reflect behavior of a portion of the arteriolar network that contributes a substantial fraction of total vascular resistance (27, 34).

### *Temporal Variations in Cell-Free Layer Width*

One of the principal and unique findings of this study is the substantial temporal variation in width of the cell-free layer as shown in Figs. 3, 7, and 8. These variations range from 30% to 70% of the layer width, depending on the diameter of the arteriole. The temporal variations increase as diameter increases and as pseudoshear rate decreases. However, a relationship to pseudoshear rate may be secondary to its dependence on diameter shown in Fig. 2. In vitro studies (37, 38) suggest that pseudoshear rate in the range of our study would not influence variability.

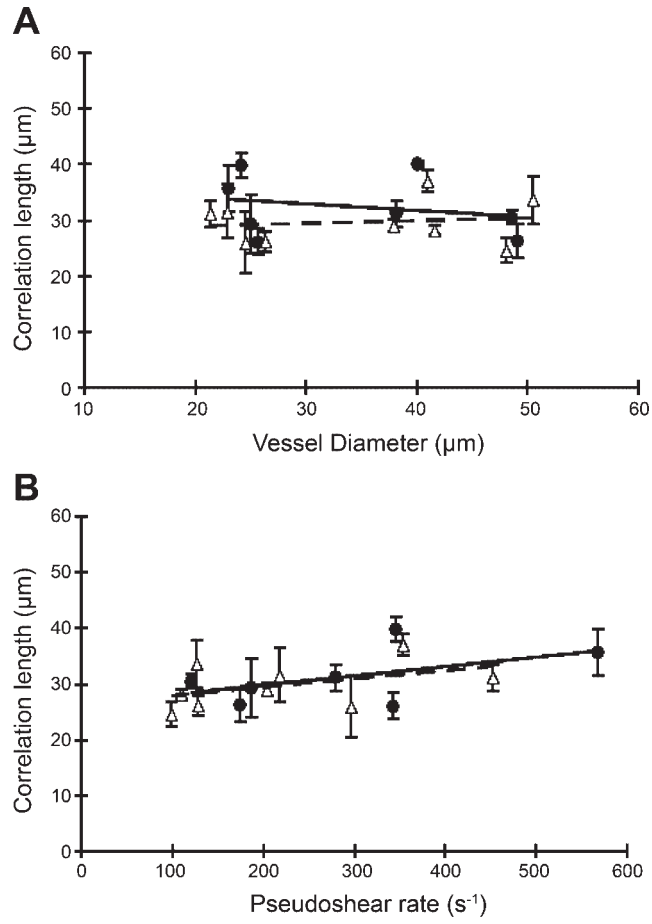


Fig. 6. Correlation length as a function of arteriolar diameter and pseudoshear rate before (●) and after (△) dextran infusion. *A*: correlation length vs. vessel diameter. *B*: correlation length vs. pseudoshear rate. There was no significant relation between correlation length and vessel diameter or pseudoshear rate either before or after dextran infusion or when the 2 groups were combined.

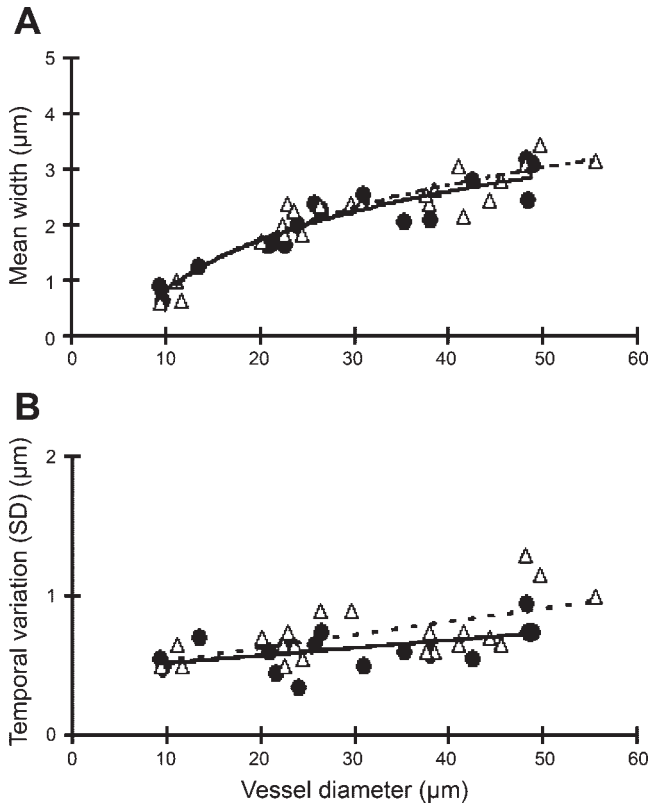


Fig. 7. Cell-free layer width as a function of arteriolar diameter in the range of 10–50 μm before (●) and after (△) dextran infusion. *A*: mean width of the cell-free layer. Logarithmic functions provided slightly better fits than linear functions. $y = 1.27\ln x - 2.10$, $R^2 = 0.86$ before dextran infusion and $y = 1.41\ln x - 2.47$, $R^2 = 0.88$ after dextran infusion. The relation between the mean width of cell-free layer and vessel diameter was highly significant ($P < 0.0001$). *B*: temporal variation expressed as SD of the cell-free layer width during a 1-s period ($n = 4{,}500$). $y = 0.01x + 0.46$, $R^2 = 0.26$ before dextran infusion. $y = 0.01x + 0.44$, $R^2 = 0.37$ after dextran infusion. The temporal variation also was significantly related ($P < 0.05$) to vessel diameter, but Dextran 500 had no significant effect.

### *Possible Errors in Measurement*

Temporal variations in vessel diameter may have contributed to the apparent changes in the cell-free layer width. Because the measurement period is brief, active changes in diameter during this time would have been small. The active autoregulatory responses of arterioles (mean diameter 36.5 μm) following arterial pressure change averaged ~0.3% during a 1-s period (17). However, it is unlikely that active changes were occurring because we did not observe periodic vasomotion or any other noticeable changes in vessel diameter during our studies.

However, passive changes in diameter may occur during the arterial pulse. Although the low contrast between the vessel wall and surrounding tissue in the cremaster preparation made it impractical to apply our method to rapid variations of vessel diameter, data in a study by Intaglietta and Tomkins (16) indicate mean diameter changes of approximately ±0.3% during the pulse in arterioles of the omentum (where visibility of the vessel wall is more favorable). This suggests that ~3% of the temporal change in 10-μm arterioles and 9% of that in 50-μm arterioles shown in Fig. 7*B* might be due to changes in vessel diameter.

Variations in velocity during the measurement would show up as apparent changes in the longitudinal dimension of the cell-free layer. A previous study (14) reported that, during the cardiac cycle, centerline velocity varied by a maximum of ±6%–7% from the mean value in arterioles of cat omentum. With the assumption that velocity changes near the wall are proportional to those at the centerline, the actual variations of the cell-free layer in the direction of flow may differ from our values by a maximum of ±6–7%.

### *Physiological Effects of Temporal Variations*

Temporal changes in the cell-free layer may be of physiological significance. A previous theoretical study (40) showed that these variations increase the effective viscosity of the cell-free layer. As shown in that study, the effect of the variations is dependent on both the nature of the pattern and the magnitude of the variations. We found that the variations in cell-free layer width are non-Gaussian (Fig. 3). This is not surprising because the outward variations are limited by the vessel wall, whereas inward variations can extend into the red blood cell core. The difference between mean and median values is not large, averaging 0.1–0.2 μm. As a consequence, the rheological effect of the departure from a Gaussian distribution may be modest.

Temporal changes would also be expected to influence the degree of scavenging of NO released from the endothelium by

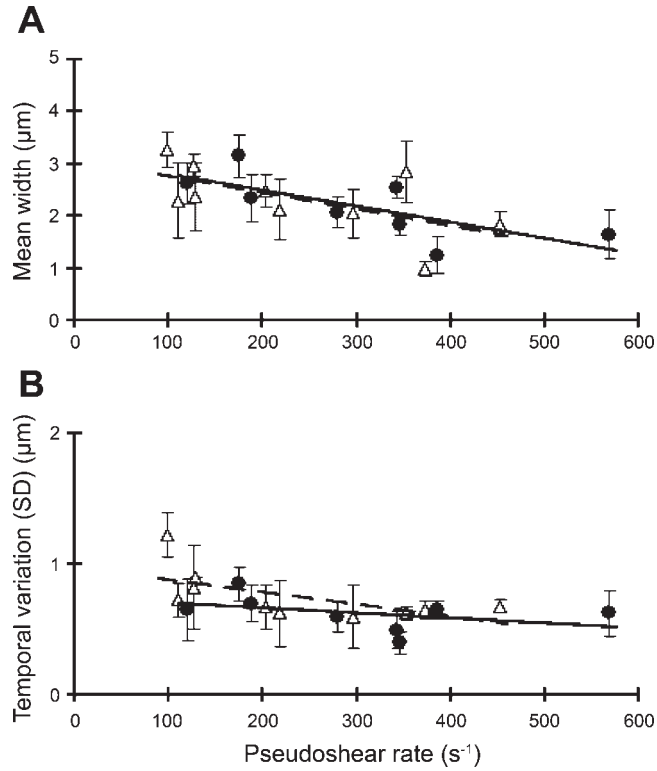


Fig. 8. Relation between pseudoshear rate and the width and variation of the cell-free layer before (●) and after (△) dextran infusion. *A*: mean width of the cell-free layer. *B*: temporal variation expressed as SD of the cell-free layer width for each vessel. There was no significant relation between pseudoshear rate and mean or temporal variation of the cell-free layer width before or after infusion of dextran. However, when the 2 groups were combined, reduction of pseudoshear rate significantly decreased ($P < 0.03$) the mean and temporal variation of the cell-free layer width.

the red blood cell core. Chen et al. (7) reported that the addition of red blood cells to a 2-μm cell-free layer would decrease the predicted peak NO in the endothelium by 21%. From that observation, temporal variations of the cell-free layer may significantly influence scavenging of NO by red blood cells in microcirculatory vessels. Because that analysis also indicated that the $P_{O_2}$ gradient is much less affected by the cell-free layer, variations in $P_{O_2}$ may not be significant.

The magnitude of the temporal variations of the cell-free layer increases as a function of vessel diameter as shown in Fig. 7*B*. This was expected because the mean width of the cell-free layer increased with vessel diameter, as shown in Fig. 7*A*. The wider cell-free layer would allow a higher degree of variability of the cell-free layer width. The variations in the cell-free layer width are not significantly affected by increasing red blood cell aggregability because the shear rates near the wall would be too high for aggregate formation. In some cases, it appears that the red blood cells approach the vessel wall within the limits of resolution of the system (~0.4 μm) as seen in Fig. 3*A*. This would place the red blood cell edge within the region of the glycocalyx, which is estimated, at a minimum, to be 0.4–0.5 μm (9, 29, 48). However, because this approach is infrequent (<2% probability in Fig. 3*A*), the hemodynamic effect may not be significant.

### *Nonaxisymmetric Nature of Cell-Free Layer Variations on Opposite Sides of the Arteriole*

We found that variations in cell-free layer width on the two sides of the flow stream are inversely related as shown in Figs. 3 and 4. This led to a small difference of ~0.5 μm in the mean width of the two layers. It should be noted that we compared not only the means of the cell-free layer width but also patterns of its temporal variation. The latter was used for correlation of the cell-free layer width on the opposite sides, which revealed a significant inverse relation. The inverse relation reflects an asymmetric boundary of the red blood cell core. The most likely explanation is lateral movements of the red blood cell column. Upstream flow conditions may affect the width of the cell-free layer on both sides of the arterioles (11). Pries et al. (35) reported that a distance of ~10 vessel diameters from an asymmetric upstream bifurcation was required for reestablishment of an axisymmetric hematocrit profile. However, such bifurcations were found in only 12% of cases. In our study, a difference of ~0.5 μm in the mean width of the cell-free layers on the two sides of the vessel was observed, indicating a possible small effect of upstream bifurcations on the cell-free layer.

It is also notable that this inverse relationship is significantly lower with increased aggregability. Considering the high pseudoshear rates in these arterioles, aggregates could form only in the very center of the flow stream where shear stress is lowest. Thus the weaker relation may be due to a stabilizing influence of red blood cell aggregation in the center of the flow stream on the lateral variations. Alternatively, the increased plasma viscosity with addition of Dextran 500 may be responsible. Additional studies would be required to resolve this question.

The inverse relationship is of potential physiological significance. Previous theoretical studies (10, 39) have shown that a nonaxisymmetric red blood cell core would increase effective blood viscosity in microcirculatory vessels, although these studies concentrated on lower pseudoshear rates than in the present study. Thus the present finding indicates that asymmetry of the flow stream increases arteriolar vascular resistance, although the magnitude of the effect cannot be assessed from information currently available. Because dextran 500 significantly decreased the nonaxisymmetry, it appears that red blood cell aggregability at normal human levels would attenuate this effect on arteriolar vascular resistance.

### *Persistence of Temporal Variations in the Cell-Free Layer Downstream*

The variations in width of the cell-free layer persist downstream in a decremental fashion as shown in Fig. 5, reflecting the mixing at the interface between the plasma layer and the red blood cell core. We found that the correlation length was ~30 μm and was not dependent on arteriolar diameter (Fig. 6*A*). A reduction of the correlation length could be expected as the vessel diameter increased since the variability of the cell-free layer increased with diameter (Fig. 7*B*). However, mean cellular velocity also increases as vessel diameter increases, which would increase the correlation length. Thus the correlation length may not be dependent on either vessel diameter or pseudoshear rate when these factors are inversely related as in the present study. The correlation length is twice that found by Silva and Intaglietta (41) (~16 μm) who performed a cross-correlation analysis of photometric signals in the centerline of a 25-μm ID arteriole at a pseudoshear rate of 124 $s^{-1}$. The higher value in our study was unexpected because the shear rate is much higher at the periphery of the flow stream and should lead to more rapid mixing than in the center of the flow stream. However, the signal recorded at the centerline of the transilluminated vessel also comes from out-of-focus layers of the flow stream (2) and is generated by cells traveling at different velocities. Finally, increasing red blood cell aggregability and pseudoshear rate did not affect the length constant as shown in Fig. 6. This finding would be expected because of the high pseudoshear rates in these vessels (100–600 $s^{-1}$), which are above the range where aggregation is normally seen and are in agreement with our earlier study on red blood cell dispersion in venules at normal arterial pressure (4, 21).

### *Diameter Dependence of the Cell-Free Layer Width*

One of the principal findings of this study is that the mean width of the cell-free layer is highly dependent on the vessel diameter (Fig. 7). We also observed an inverse relation between the mean width and pseudoshear rate (Fig. 8), but this is likely secondary to a dependence of pseudoshear rate on vessel diameter. Over the diameter range 10–50 μm, the mean width rose from 0.8 to 2.9 μm. The relationship was not significantly affected by dextran infusion, probably because of the high shear rates. Previous studies on the relation between cell-free layer dimensions and diameter are limited and are not in agreement. Maeda and coworkers (43) found generally similar values of the cell-free layer width to ours, 1.1–2.1 μm, over the diameter range 10–40 μm in microvessels of the isolated rabbit mesentery perfused with human red blood cells suspended in saline at 30% hematocrit at pseudoshear rates of 150–350 $s^{-1}$. Addition of 1 g/dl Dextran 70 increased the mean width by ~0.2 μm. Similar to our findings, they also

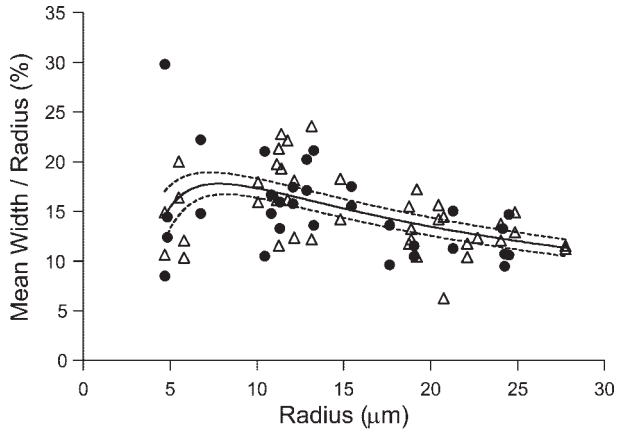


Fig. 9. Cell-free layer width as a fraction of arteriolar radius before and after dextran infusion. The solid line represents a nonlinear regression curve [$y = (1.387\ln x - 1.463)/x$, $R^2 = 0.24$] for the combined group before (●) and after (△) dextran infusion. The dashed lines indicate the 95% confidence band of the regression curve.

reported that a logarithmic relation between the mean width and the vessel diameter provided the best fit (30, 43). A saturation-type relationship between width and diameter was predicted in an earlier theoretical study (40). For arterioles in the 10- to 30-μm range, Pries et al. (35) found that the estimated mean cell-free layer width increased from ~1.2 to 1.7 μm based on red blood cell-plasma separation at bifurcations.

In vitro studies of the cell-free layer width also show a dependence on diameter. In 31- and 58-μm ID glass tubes, the mean cell-free layer thicknesses using human blood with a feed hematocrit of 45% were 2.0 and 2.9 μm, respectively, at a pseudoshear rate of 90 $s^{-1}$ (37). The comparable values based on our data would be 2.3 and 3.2 μm, respectively. Thus it appears that the cell-free layer may be slightly thinner in vitro, possibly because of the absence of the glycocalyx.

In contrast to these findings, Yamaguchi et al. (49) found a considerably greater width of the cell-free layer in vessels on the surface of the cat brain, 3.6–4.6 μm over the arteriolar diameter range 34–56 μm at pseudoshear rates >90 $s^{-1}$, which was independent of vessel diameter. The reason for higher values in the cat brain is not obvious but may relate to the use of rhodamine isothocyanate-labeled dextran in the plasma for the width of the flow stream and absorption of the excitation signal to measure the width of the red blood cell column.

*Cell-Free Layer Width as a Fraction of Vessel Radius*

To quantify the fraction of the vessel lumen occupied by the cell-free layer, the data shown in Fig. 7*A* are expressed as a function of vessel radius in Fig. 9. Because there was no significant difference in the data shown in Fig. 7*A* before and after dextran infusion, the two groups were combined for this analysis. We used the same logarithmic function as in Fig. 7*A* because it gave a slightly higher $R^2$ value than a linear fit (0.24 vs. 0.17). Although the absolute width of the cell-free layer increased with vessel diameter as shown in Fig. 7*A*, the cell-free layer width as a fraction of vessel radius increased slightly in the range of 5–8 μm but gradually decreased as the radius increased from 8 to 25 μm, with the mean value falling from 18% to 12%. Thus it appears that the cell-free layer occupied the greatest fraction of the lumen in arterioles of ~16-μm internal diameter. In those vessels, the cell-free layer would occupy ~33% of the cross-sectional area of the lumen; this value falls to ~23% in 50-μm ID arterioles. The data scatter in the cell-free layer to radius ratio is likely due to several factors, including measurement error, particularly in the smallest vessels, effects of upstream bifurcations (11), and variability of hematocrit (28). The latter has been shown to be an important determinant of cell-free layer width (30, 40, 45).

Figure 9 reveals two opposing trends in the cell-free layer width when it is normalized to vessel radius, which are not apparent when absolute values are compared (Fig. 7). As radius increases from 8 to 25 μm, the cell-free layer decreases as a fraction of vessel radius. Reduction of pseudoshear rate with increased radius (Fig. 2) would reduce the normalized axial migration of red blood cells, as would the increased hematocrit. The reduction in pseudoshear rate and increased hematocrit are apparently not sufficient to decrease the absolute width when radius increases (Fig. 7). The opposite trend in the vessels of 5- to 8-μm radius may reflect a transient range changing from a single-file to multifile flow of red blood cells and the contribution of the glycocalyx to the measured value of the cell-free layer as discussed further below.

*Contribution of the Glycocalyx to the Cell-Free Layer*

The thickness of the glycocalyx is included in the width of the cell-free layer in the present study. Considering a glycocalyx layer of 0.4–0.5 μm as previously reported by Damiano and coworkers in venules and by Vink and Duling in capillaries (9, 29, 48), 10-μm and 50-μm arterioles would have a free-flowing layer of 0.3–0.4 μm and 2.6–2.7 μm, respectively. Subtraction of the glycocalyx leads to prediction of a very thin free-flowing layer in 10-μm arterioles. On the basis of microvascular network hemodynamic data, Pries and Secomb (36) calculated the width of the endothelial surface layer (ESL) to be a biphasic function of arteriolar diameter with an initial peak of ~0.8 μm in 10-μm arterioles, increasing to ~1 μm in 50-μm vessels. With the use of their estimate of the ESL width, the free-flowing layer width would be reduced significantly. Their value for the ESL width in 10-μm arterioles is essentially equal to the width of the cell-free layer in our study. However, the flow regimen in these vessels might be quite different from that in larger vessels (12), being a single-file or a tandem (slipper) arrangement of overlapping red blood cells as opposed to the multifile flow in the larger vessels. Therefore, the hemodynamic effects of the width of the cell-free layer in the 10-μm arterioles cannot be readily compared with those in larger arterioles. In addition, our data on cell-free layer width, especially in the smallest arterioles, must be interpreted with some caution because spatial resolution with our system is ~0.4 μm, which is half the width of the cell-free layer in the 10-μm arterioles.

*Physiological Importance of Mean Cell-Free Layer Width*

Available evidence suggests that an increase in mean thickness of the cell-free layer may reduce vascular resistance. Maeda and coworkers (30, 43) reported that increasing cell-free layer width by elevation of red blood cell aggregability with infusion of dextran 70 substantially reduced flow resis-

tance in microvessels. Also, Sharan and Popel (40) predicted that relative viscosity near the wall of a 50-μm vessel would increase by ~15% when the cell-free layer width fell from ~4.3 to 3 μm with an increase of systemic hematocrit from 45% to 60%.

A second physiological consequence would be a change in the NO scavenging effect of the red blood cell core. As noted in the Introduction, Liao et al. (25) showed that, during flow, the scavenging of NO by red blood cells in the vessel lumen of isolated, blood-perfused arterioles was greatly reduced, presumably because of the presence of the cell-free layer. A theoretical study by Lamkin-Kennard et al. (24) indicated that a change in width of the layer by 2 μm would change NO scavenging by 40%. The diameter dependence of the cell-free layer width in our study would lead to a lower scavenging effect of red blood cells on NO release from the endothelial layer in the larger arterioles (6, 47). This may influence the contribution of NO to regulation of arteriolar vascular tone at different levels of the arteriolar network.

We also note that the diameter dependence of the cell-free layer may modify changes in vascular tone induced by regulatory mechanisms. During vasoconstriction, for example, the reduction in cell-free layer width would increase the NO scavenging effect of the red blood cells, whereas during vasodilation an increase in layer width would decrease scavenging. The same changes in cell-free layer width would have an opposite effect on regulatory mechanisms by increasing wall shear stress during constriction and decreasing it during dilation. The width of the layer may also influence expression of regulatory mechanisms. Baskurt et al. (3) reported that increasing the aggregability of red blood cells led to a decrease in endothelial NO synthase formation in small arteries, presumably due to an increase in width of the cell-free layer and reduction of wall shear stress.

### *Conclusions*

*1*) The mean width of the cell-free layer in rat cremaster arterioles is directly related to the vessel diameter, increasing from 0.8 μm in 10-μm arterioles to 2.9 μm in 50-μm arterioles. Temporal variations also increase as diameter increases. The variation is not normally distributed, being greater toward the center of the flow stream, but the effect is small.

*2*) Temporal variations in the cell-free layer on the two sides of the arteriole are inversely related, possibly due to lateral movements of the red blood cell column. This relationship introduces asymmetry in red blood cell distribution near the wall and may increase effective blood viscosity.

*3*) The temporal variations of the cell-free layer seen at a specific point in an arteriole decline exponentially downstream with a correlation length (~30 μm) that is independent of vessel diameter and of pseudoshear rate at normal pseudoshear rates.

*4*) Increasing red blood cell aggregability to normal human levels with dextran 500 infusion has no effect on the cell-free layer width or variations at normal pseudoshear rates (100 to 500 $s^{-1}$) but does significantly reduce the inverse relation cited in *point 2* above, possibly indicating a reduction of lateral movements of the red blood cell column. This would attenuate effects of asymmetry on effective viscosity.

## ACKNOWLEDGMENTS

The authors thank Scott Dunning and Janet Zhen for expert technical assistance.

## GRANTS

This work was supported by National Heart, Lung, and Blood Institute Grants HL-52684, HL-62318, and HL-64395.

## REFERENCES

1. **Baez S.** An open cremaster muscle preparation for the study of blood vessels by in vivo microscopy. *Microvasc Res* 5: 384–394, 1973.
2. **Baker M, Wayland H.** On-line volume flow rate and velocity profile measurement for blood in microvessels. *Microvasc Res* 7: 131–143, 1974.
3. **Baskurt OK, Yalcin O, Ozdem S, Armstrong JK, Meiselman HJ.** Modulation of endothelial nitric oxide synthase expression. *Am J Physiol Heart Circ Physiol* 286: H222–H229, 2004.
4. **Bishop JJ, Popel AS, Intaglietta M, Johnson PC.** Effect of aggregation and shear rate on the dispersion of red blood cells flowing in venules. *Am J Physiol Heart Circ Physiol* 283: H1985–H1996, 2002.
5. **Busse R, Fleming I.** Regulation of endothelium-derived vasoactive autacoid production by hemodynamic forces. *Trends Pharmacol Sci* 24: 24–29, 2003.
6. **Butler AR, Megson IL, Wright PG.** Diffusion of nitric oxide and scavenging by blood in the vasculature. *Biochim Biophys Acta* 1425: 168–176, 1998.
7. **Chen X, Jaron D, Barbee KA, Buerk DG.** The influence of radial RBC distribution, blood velocity profiles, and glycocalyx on coupled $NO/O_2$ transport. *J Appl Physiol* 100: 482–492, 2006.
8. **Cokelet GR, Goldsmith HL.** Decreased hydrodynamic resistance in the two-phase flow of blood through small vertical tubes at low flow rates. *Circ Res* 68: 1–17, 1991.
9. **Damiano ER.** The effect of the endothelial-cell glycocalyx on the motion of red blood cells through capillaries. *Microvasc Res* 55: 77–91, 1998.
10. **Das B, Johnson PC, Popel AS.** Effect of nonaxisymmetric hematocrit distribution on non-Newtonian blood flow in small tubes. *Biorheology* 35: 69–87, 1998.
11. **Enden G, Popel AS.** A numerical study of plasma skimming in small vascular bifurcations. *J Biomech Eng* 116: 79–88, 1994.
12. **Gaehtgens P, Duhrssen C, Albrecht KH.** Motion, deformation, and interaction of blood cells and plasma during flow through narrow capillary tubes. *Blood Cells* 6: 799–817, 1980.
13. **Gretz JE, Duling BR.** Measurement uncertainties associated with the use of bright-field and fluorescence microscopy in the microcirculation. *Microvasc Res* 49: 134–140, 1995.
14. **Intaglietta M, Richardson DR, Tompkins WR.** Blood pressure, flow, and elastic properties in microvessels of cat omentum. *Am J Physiol* 221: 922–928, 1971.
15. **Intaglietta M, Silverman NR, Tompkins WR.** Capillary flow velocity measurements in vivo and in situ by television methods. *Microvasc Res* 10: 165–179, 1975.
16. **Intaglietta M, Tompkins WR.** On-line measurement of microvascular dimensions by television microscopy. *J Appl Physiol* 32: 546–551, 1972.
17. **Johnson PC.** Autoregulatory responses of cat mesenteric arterioles measured in vivo. *Circ Res* 22: 199–212, 1968.
18. **Johnson PC, Intaglietta M.** Contributions of pressure and flow sensitivity to autoregulation in mesenteric arterioles. *Am J Physiol* 231: 1686–1698, 1976.
19. **Kavdia M, Tsoukias NM, Popel AS.** Model of nitric oxide diffusion in an arteriole: impact of hemoglobin-based blood substitutes. *Am J Physiol Heart Circ Physiol* 282: H2245–H2253, 2002.
20. **Kim S, Kong RL, Popel AS, Intaglietta M, Johnson PC.** A computer-based method for determination of the cell-free layer width in the microcirculation. *Microcirculation* 13: 199–207, 2006.
21. **Kim S, Popel AS, Intaglietta M, Johnson PC.** Aggregate formation of erythrocytes in postcapillary venules. *Am J Physiol Heart Circ Physiol* 288: H584–H590, 2005.
22. **Kim S, Popel AS, Intaglietta M, Johnson PC.** Effect of erythrocyte aggregation at normal human levels on functional capillary density in rat spinotrapezius muscle. *Am J Physiol Heart Circ Physiol* 290: H941–H947, 2006.
23. **Koller A, Kaley G.** Prostaglandins mediate arteriolar dilation to increase blood flow velocity in skeletal muscle microcirculation. *Circ Res* 67: 529–534, 1990.

24. **Lamkin-Kennard KA, Jaron D, Buerk DG.** Impact of the Fahraeus effect on NO and $O_2$ biotransport: a computer model. *Microcirculation* 11: 337–349, 2004.
25. **Liao JC, Hein TW, Vaughn MW, Huang KT, Kuo L.** Intravascular flow decreases erythrocyte consumption of nitric oxide. *Proc Natl Acad Sci USA* 96: 8757–8761, 1999.
26. **Lipowsky HH.** Mechanics of blood flow in the microcirculation. In: *Handbook of Bioengineering*, edited by Skalak R, Chien S. New York: McGraw-Hill, 1986.
27. **Lipowsky HH, Kovalcheck S, Zweifach BW.** The distribution of blood rheological parameters in the microvasculature of cat mesentery. *Circ Res* 43: 738–49, 1978.
28. **Lipowsky HH, Usami S, Chien S.** In vivo measurements of "apparent viscosity" and microvessel hematocrit in the mesentery of the cat. *Microvasc Res* 19: 297–319, 1980.
29. **Long DS, Smith ML, Pries AR, Ley K, Damiano ER.** Microviscometry reveals reduced blood viscosity and altered shear rate and shear stress profiles in microvessels after hemodilution. *Proc Natl Acad Sci USA* 101: 10060–10065, 2004.
30. **Maeda N, Suzuki Y, Tanaka J, Tateishi N.** Erythrocyte flow and elasticity of microvessels evaluated by marginal cell-free layer and flow resistance. *Am J Physiol Heart Circ Physiol* 271: H2454–H2461, 1996.
31. **Marton Z, Kesmarky G, Vekasi J, Cser A, Russai R, Horvath B, Toth K.** Red blood cell aggregation measurements in whole blood and in fibrinogen solutions by different methods. *Clin Hemorheol Microcirc* 24: 75–83, 2001.
32. **Motulsky H.** *Prism 4 Statistics Guide: Statistical Analyses for Laboratory And Clinical Researchers.* San Diego, CA: GraphPad Software, 2003.
33. **Olson JS, Foley EW, Rogge C, Tsai AL, Doyle MP, Lemon DD.** NO scavenging and the hypertensive effect of hemoglobin-based blood substitutes. *Free Radic Biol Med* 36: 685–697, 2004.
34. **Popel AS, Johnson PC.** Microcirculation and hemorheology. *Annu Rev Fluid Mech* 37: 43–69, 2005.
35. **Pries AR, Ley K, Claassen M, Gaehtgens P.** Red cell distribution at microvascular bifurcations. *Microvasc Res* 38: 81–101, 1989.
36. **Pries AR, Secomb TW.** Microvascular blood viscosity in vivo and the endothelial surface layer. *Am J Physiol Heart Circ Physiol* 289: H2657–H2664, 2005.
37. **Reinke W, Gaehtgens P, Johnson PC.** Blood viscosity in small tubes: effect of shear rate, aggregation, and sedimentation. *Am J Physiol Heart Circ Physiol* 253: H540–H547, 1987.
38. **Reinke W, Johnson PC, Gaehtgens P.** Effect of shear rate variation on apparent viscosity of human blood in tubes of 29 to 94 μm diameter. *Circ Res* 59: 124–132, 1986.
39. **Secomb TW, el-Kareh AW.** A model for motion and sedimentation of cylindrical red-cell aggregates during slow blood flow in a narrow horizontal tubes. *J Biomech Eng* 116: 243–249, 1994.
40. **Sharan M, Popel AS.** A two-phase model for flow of blood in narrow tubes with increased effective viscosity near the wall. *Biorheology* 38: 415–428, 2001.
41. **Silva J, Intaglietta M.** The correlation of photometric signals derived from in vivo red blood cell flow in microvessels. *Microvasc Res* 7: 156–169, 1974.
42. **Smith ML, Long DS, Damiano ER, Ley K.** Near-wall μ-PIV reveals a hydrodynamically relevant endothelial surface layer in venules in vivo. *Biophys J* 85: 637–645, 2003.
43. **Soutani M, Suzuki Y, Tateishi N, Maeda N.** Quantitative evaluation of flow dynamics of erythrocytes in microvessels: influence of erythrocyte aggregation. *Am J Physiol Heart Circ Physiol* 268: H1959–H1965, 1995.
44. **Suzuki Y, Tateishi N, Soutani M, Maeda N.** Flow behavior of erythrocytes in microvessels and glass capillaries: effects of erythrocyte deformation and erythrocyte aggregation. *Int J Microcirc Clin Exp* 16: 187–194, 1996.
45. **Tateishi N, Suzuki Y, Cicha I, Maeda N.** $O_2$ release from erythrocytes flowing in a narrow $O_2$-permeable tube: effects of erythrocyte aggregation. *Am J Physiol Heart Circ Physiol* 281: H448–H456, 2001.
46. **Tateishi N, Suzuki Y, Soutani M, Maeda N.** Flow dynamics of erythrocytes in microvessels of isolated rabbit mesentery: cell-free layer and flow resistance. *J Biomech* 27: 1119–1125, 1994.
47. **Vaughn MW, Kuo L, Liao JC.** Effective diffusion distance of nitric oxide in the microcirculation. *Am J Physiol Heart Circ Physiol* 274: H1705–H1714, 1998.
48. **Vink H, Duling BR.** Identification of distinct luminal domains for macromolecules, erythrocytes, and leukocytes within mammalian capillaries. *Circ Res* 79: 581–589, 1996.
49. **Yamaguchi S, Yamakawa T, Niimi H.** Cell-free plasma layer in cerebral microvessels. *Biorheology* 29: 251–260, 1992.
50. **Zhao H, Wang X, Stoltz JF.** Comparison of three optical methods to study erythrocyte aggregation. *Clin Hemorheol Microcirc* 21: 297–302, 1999.